Supplementary Information (SI) for Journal of Materials Chemistry A.

Supporting Information

Nanorods Assembled Urchin-like Molybdenum-Manganese Oxide Heterostructure with Enhanced Oxygen Vacancies as Cathode for Quasi Solid State Zinc-ion Batteries

Jianjiang Mao, Xinxin Li, Yu Huang, Chengyu Zhu, Fengshou Yu, Fei Cheng*

School of Chemical Engineering and Technology, Hebei University of Technology, Xiping Road 5340, Beichen District, Tianjin 300130, China.

* Corresponding author. E-mail address: fcheng@hebut.edu.cn

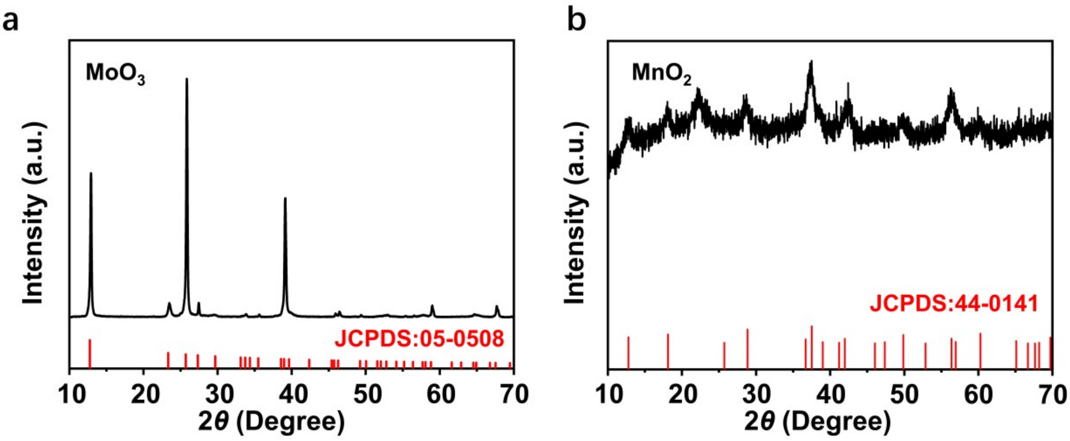

Figure S1. The XRD patterns of a) MoO_3 and b) MnO_2

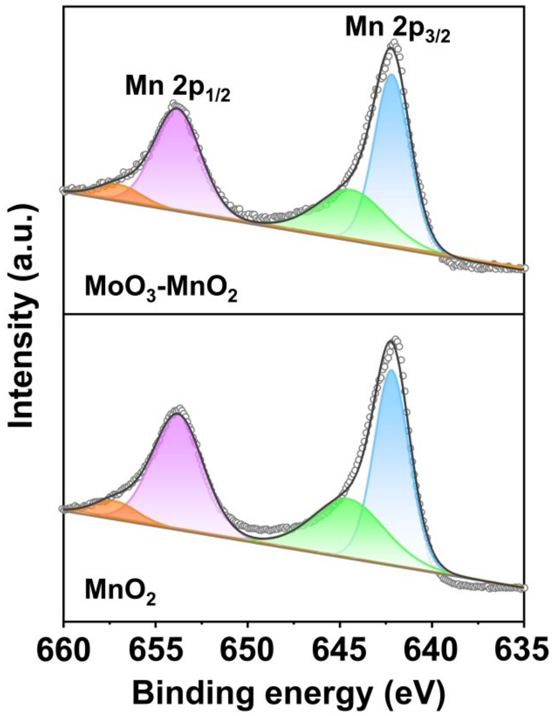

Figure S2. Mn 2p XPS spectra of MnO_2 and MoO_3-MnO_2

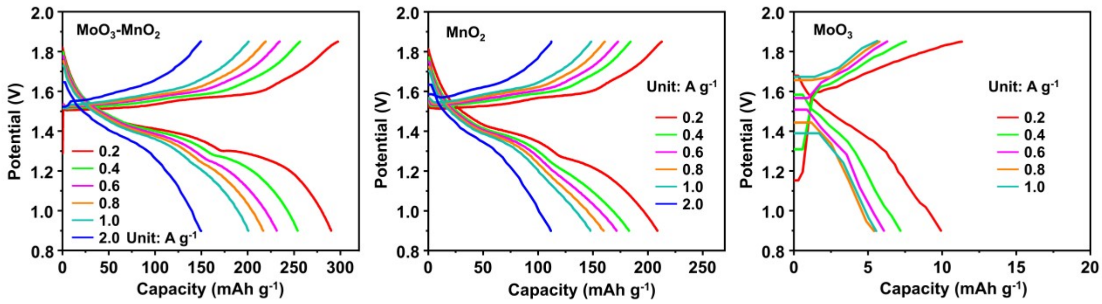

Figure S3. The charging and discharging curves at various current densities for a) MoO_3-MnO_2, b) MnO_2 and c) MoO_3

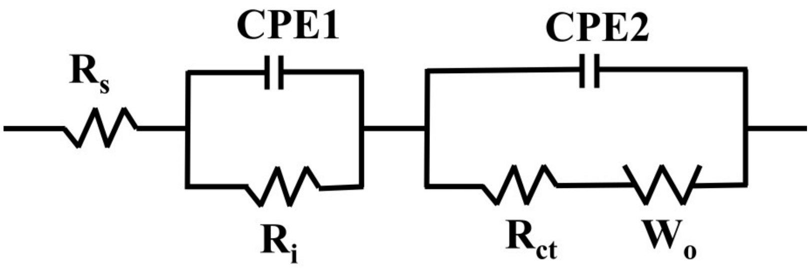

Figure S4. The equivalent circuit diagram of samples

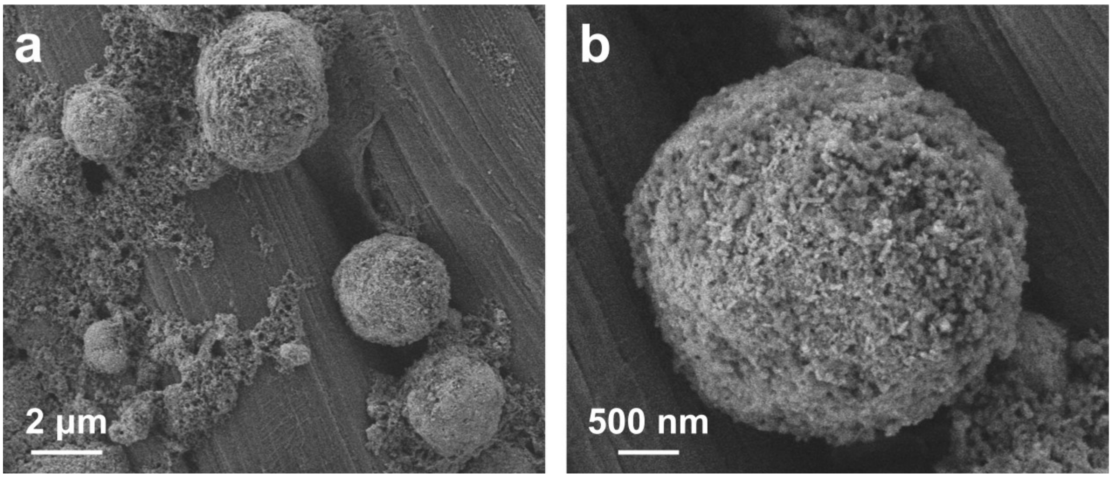

Figure S5. SEM images of MoO_3-MnO_2 electrode after 1000 cycles

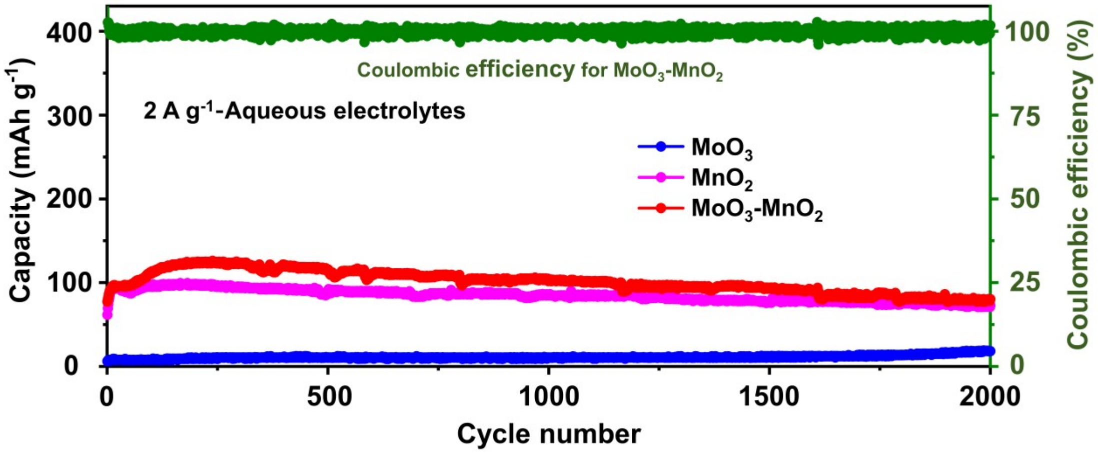

Figure S6. The cycling performance of MoO_3, MnO_2, and MoO_3-MnO_2 at 2 A g^{-1} in aqueous electrolytes

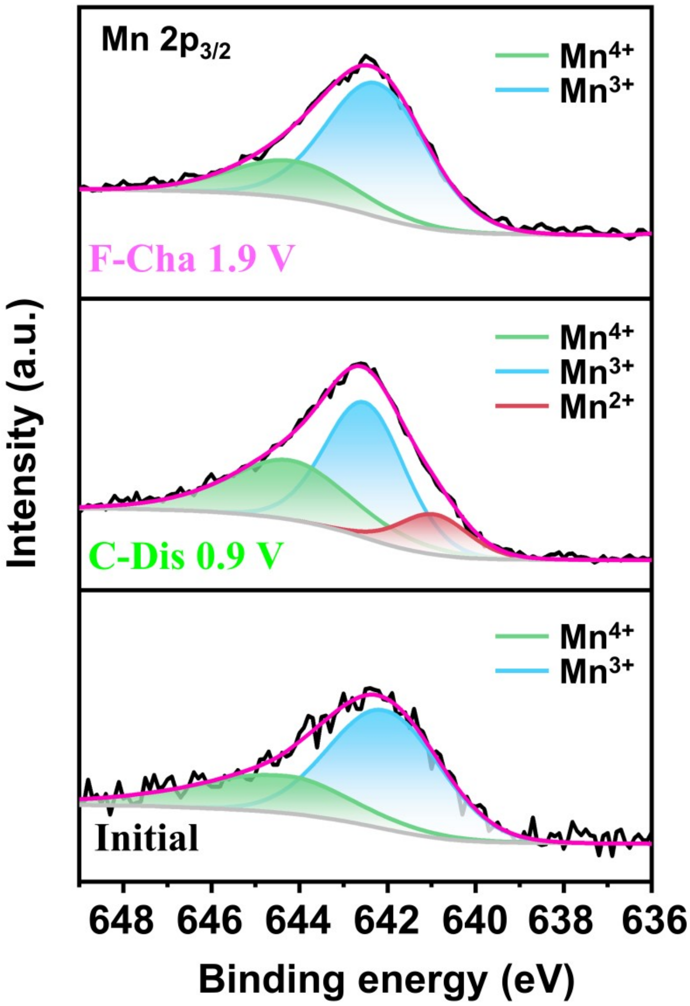

Figure S7. Mn $2p_{3/2}$ ex-situ high-discern XPS spectra of MoO_3-MnO_2

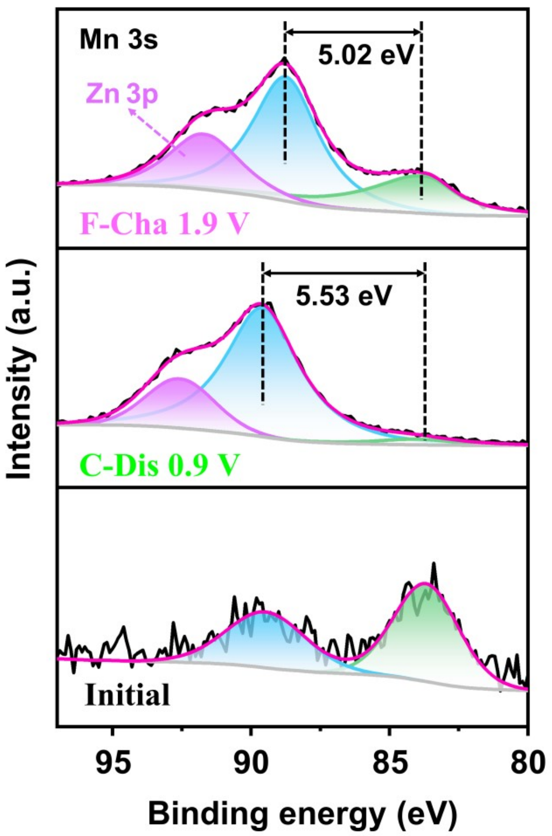

Figure S8. Mn 3s ex-situ high-discern XPS spectra of MoO_3-MnO_2

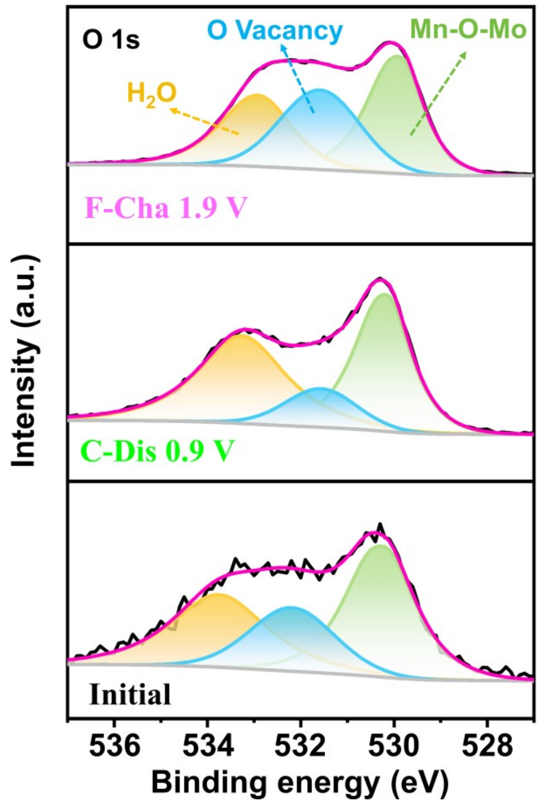

Figure S9. O 1s ex-situ high-discern XPS spectra of MoO_3-MnO_2

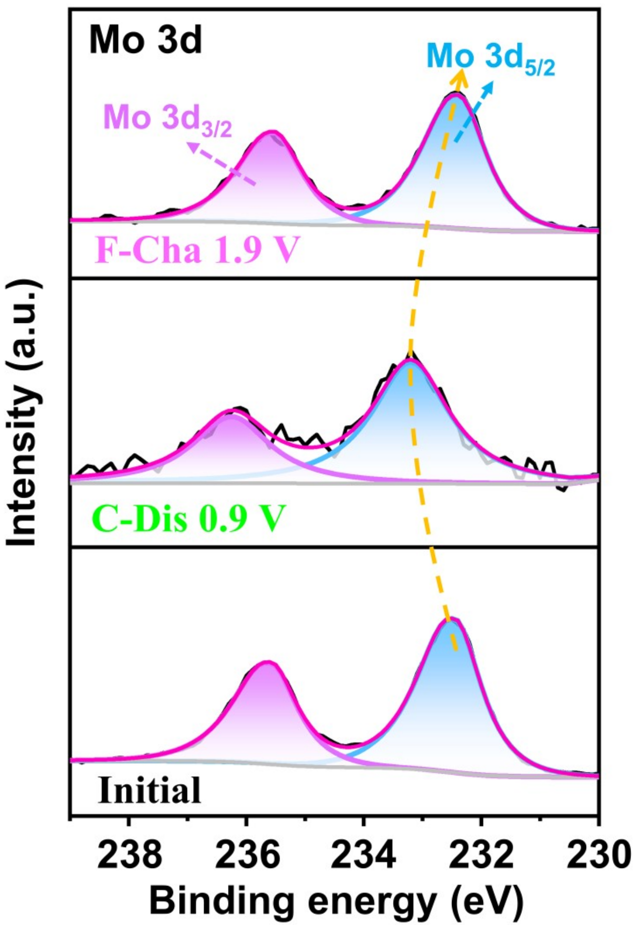

Figure S10. Mo 3d ex-situ high-discern XPS spectra of MoO_3-MnO_2

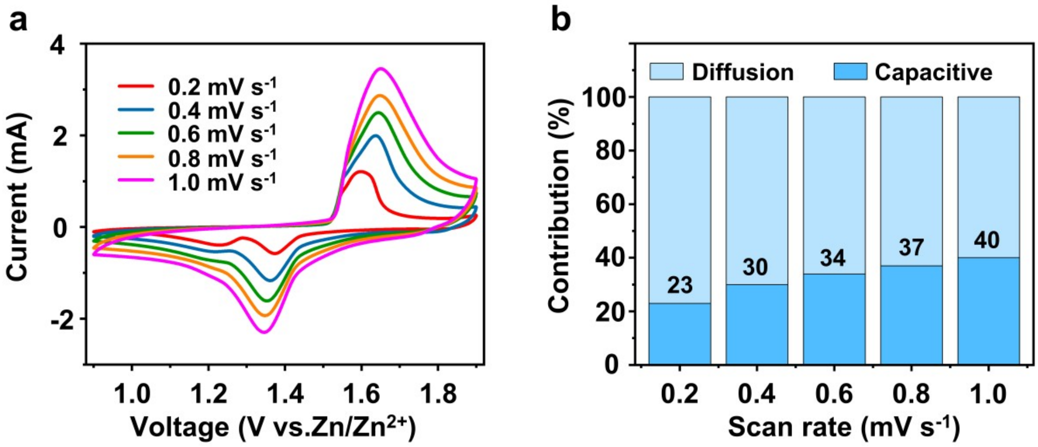

Figure S11. a) CV curves of the pure MnO_2 electrode at different scan rates, b) Contribution ratios of the capacitive and diffusion-controlled capacities at different scan rates

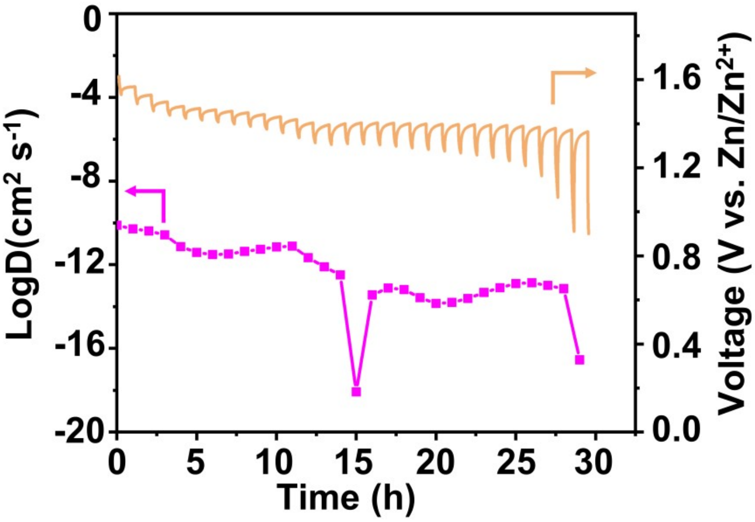

Figure S12. GITT of the MnO_2 electrode

The calculation of Diffusion coefficient

The Zn//MnO_2 and Zn//MoO_3-MnO_2 batteries were discharged at 0.1 A g^{-1} for 10 min and then relaxed for 1 h, which repeated the above operation from 0.9 V to 1.9 V. The specific calculation is as follows:

$$D = \frac{4}{\pi \Delta\tau}\left(\frac{m_B V_M}{M_B S}\right)^2\left(\frac{\Delta E_s}{\Delta E_\tau}\right)^2$$

Where τ is the pulse duration; m_B, V_M, and M_B are the mass, molar volume, and molar mass of active materials; S is the area in contact with electrolytes; ΔEs and ΔEτ represent the voltage change caused by the pulse and the voltage change of constant current charge-discharge, respectively.

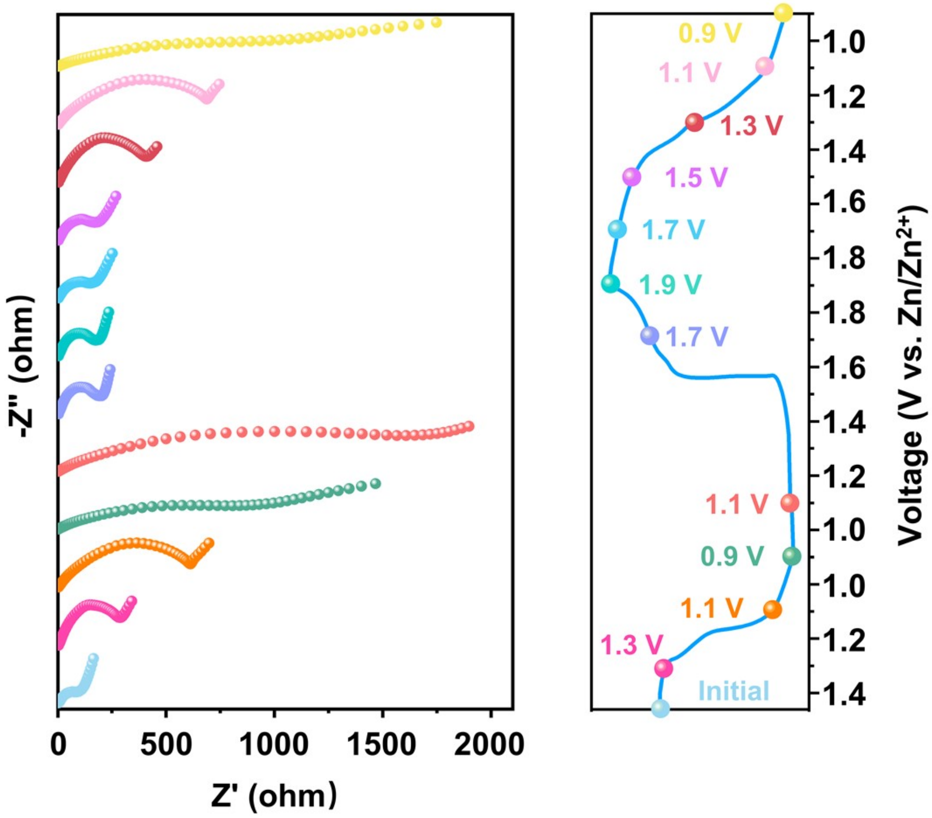

Figure S13. Nyquist plots for MoO_3-MnO_2 cathode during the discharge and charge process

Table S1. Fitting results of R_s and R_{ct} of the EIS based on the equivalent circuit. The ion diffusion coefficient was calculated based on EIS

	R_s(Ω)	**R_{ct}(Ω)**	**Diffusion coefficient（cm^2 s^{-1}）**
MoO_3	4.452	101.9	2.98×10^{-12}
MnO_2	2.048	55.75	1.25×10^{-11}
MoO_3-MnO_2	2.123	39.6	2.71×10^{-11}

Table S2. Comparison of cathode performance in AZIBs between this work and previously reported

Cathode Materials	Specific capacity mAh g^{-1}@A g^{-1}	Capacity after cycling (mAh g^{-1}@ A g^{-1}) (Cycle number)	Rate performance (mAh g^{-1})		Ref.
			1 A g^{-1}	2 A g^{-1}	
MoO_3-MnO_2	**319@0.2**	**155@1 (1000)** **116@2 (2000)**	**201**	**150**	**This work**
β-$MnO_2(O_d)$	307@0.1	169@1 (800)	195	154	[1]
SbMO-6	276@0.1	113@2 (2000)	192	171	[2]

$NiCo_2O_4$-MnO_2	313@0.1	192@1 (1000)	202	—	3
α-MnO_2/ γ-MnO_2	278@0.1	65@3 (2800)	134	—	4
CaMnO	260@0.3	140@1.5 (750)	193	104	5
1.05 KCl-MnO_2	275@0.1	96@1 (1000)	109	—	6
a-H-MnFeO	247@0.2	~135@1 (1000)	109	50	7
Ti-$Na_{0.44}MnO_2$	252@0.05	~90@1 (2400)	110	—	8
Pr_6O_{11}-Mn_2O_3	347@0.1	140.8@1 (2000)	197	186	9

Reference

1. J. Zheng, C. Qin, C. Chen, C. Zhang, P. Shi, X. Chen, Y. Gan, J. Li, J. Yao, X. Liu, J. Cheng, D. Sun, H. Wan and H. Wang, *Journal of Materials Chemistry A*, 2023, **11**, 24311-24320.
2. H. Huang, H. Feng, Z. He, Y. Huang, J. Xu, C. Hu, Z. Chen, Z. Yang and W. Zhang, *ACS Nano*, 2024, **18**, 25601-25613.
3. X. Lu, L. Chen, R. Orenstein, W. Li, W. Chi, M. Peng, C. Wang, Y. Liu and X. Zhang, *Small*, 2024, 2406680.
4. K. Wang, D. Wu, X. Sun, W. Zhang, Z. Zhang, Y. Zhen, Y. Yang and J. Wang, *ACS Sustainable Chemistry & Engineering*, 2023, **11**, 15818-15825.
5. D. Xie, Y. Wang, L. Tian, H. Huang, J. Sun, D.-W. Kim, J. Zhao and J. Mao, *Adv Funct Mater*, 2024, 2413993.
6. Y. Gao, J. Zhou, L. Qin, Z. Xu, Z. Liu, L. Wang, X. Cao, G. Fang and S. Liang, *Green Energy & Environment*, 2023, **8**, 1429-1436.
7. F. Jing, C. Lv, L. Xu, Y. Shang, J. Pei, P. Song, Y. Wang, G. Chen and C. Yan, *Journal of Energy Chemistry*, 2023, DOI: 10.1016/j.jechem.2023.08.036.
8. K. Wang, G. Guo, X. Tan, L. Zheng and H. Zhang, *Chemical Engineering Journal*, 2023, **451**.
9. Q. Liu, G. Fan, Y. Zeng, X. Zhang, D. Luan, Y. Guo, X. Gu and X. W. Lou, *Adv Energy Mater*, 2024, **14**, 2402743.